Published in final edited form as:
J Comp Neurol. 2012 February 15; 520(3): 606–619. doi:10.1002/cne.22753.

Reelin Demarcates a Subset of Pre-Bötzinger Complex Neurons in Adult Rat

Wenbin Tan[*], **David Sherman**, **Jenny Turesson**[*], **Xuesi M. Shao**, **Wiktor A. Janczewski**, and **Jack L. Feldman**[*]
Department of Neurobiology, David Geffen School of Medicine at UCLA, Los Angeles, California 90095

Abstract

Identification of two markers of neurons in the pre- Bötzinger complex (pre-BötC), the neurokinin 1 receptor (NK1R) and somatostatin (Sst) peptide, has been of great utility in understanding the essential role of the pre-BötC in breathing. Recently, the transcription factor dbx1 was identified as a critical, but transient, determinant of glutamatergic pre-BötC neurons. Here, to identify additional markers, we constructed and screened a single-cell subtractive cDNA library from pre-BötC inspiratory neurons. We identified the glycoprotein reelin as a potentially useful marker, because it is expressed in distinct populations of pre-BötC and inspiratory bulbospinal ventral respiratory group (ibsVRG) neurons. Reelin ibsVRG neurons were larger (27.1 ± 3.8 μm in diameter) and located more caudally (>12.8 mm caudal to Bregma) than reelin pre-BötC neurons (15.5 ± 2.4 μm in diameter, <12.8 mm rostral to Bregma). Pre-BötC reelin neurons coexpress NK1R and Sst. Reelin neurons were also found in the parahypoglossal and dorsal parafacial regions, pontine respiratory group, and ventromedial medulla. Reelin-deficient (Reeler) mice exhibited impaired respones to hypoxia compared with littermate controls. We suggest that reelin is a useful molecular marker for pre-BötC neurons in adult rodents and may play a functional role in pre- BötC microcircuits.

INDEXING TERMS

breathing; hypoxia; reelin; Ahi1; latexin; PRMC1

The pre-Bötzinger complex (pre-BötC) in the ventrolateral medulla is the hypothesized kernel for generating the normal inspiratory-dominated respiratory rhythm in vivo and its in vitro equivalent (Gray et al., 1999, 2001; Janczewski and Feldman, 2006; Smith et al., 1991), containing many different respiratory neuron types with distinctive respiratory-modulated discharge patterns (Guyenet and Wang, 2001; Schwarzacher et al., 1995). The pre-BötC and its immediate surrounding area contain neurons presumptively unrelated to generation or modulation of respiratory pattern, such as C1 adrenergic neurons and cardiovagal motor neurons (Bianchi et al., 1995; Chan and Sawchenko, 1998; Guyenet, 2000; Standish et al., 1994). Given its heterogeneity, clearly defined criteria for identifying neurons making up the pre-BötC are essential for determining their roles in respiratory motor patterning. Two molecules that identify overlapping subpopulations of glutamatergic

[*]CORRESPONDENCE TO: Jack L. Feldman, Department of Neurobiology, David Geffen School of Medicine at UCLA, Los Angeles, CA 90095-1763. feldman@ucla.edu.
Wenbin Tan's current address is Beckman Laser Institute, University of California at Irvine, Irvine, CA 92612.
Jenny Turesson's current address is Department of Pediatrics, Karolinska Institute, Stockholm, Sweden.

Additional Supporting Information may be found in the online version of this article.

pre-BötC neurons, demarcated by expression of NK1R and/or Sst have been useful in this regard: 1) Lesioning NK1R-expressing pre-BötC neurons abolishes normal breathing in adult rats (Gray et al., 2001); 2) acute silencing of Sst-expressing pre-BötC neurons produces prolonged apnea that can result in asphyxia (Tan et al., 2008). The transcription factor dbx1 is critical for proper development of glutamatergic pre-BötC neurons (Bouvier et al., 2010; Gray et al., 2010). However, each of these markers has limitations. In the pre-BötC, NK1R immunoreactivity (-ir) is localized predominantly in neuronal processes and not somata, Sst expression decreases significantly during aging (Hayashi et al., 1997; Lu et al., 2004; Tan et al., 2010), and dbx1 is expressed only prenatally in progenitor neurons (Bouvier et al., 2010; Gray et al., 2010).

Here, we sought to identify additional markers to complement and extend the utility of NK1R, Sst, and dbx1, which could be helpful in revealing the function and structure of pre-BötC neuronal microcircuitry underlying respiratory rhythm and pattern generation. To this end, we constructed and screened a subtractive cDNA library from pre-BötC inspiratory neurons and neighboring nucleus ambiguous (NA) motoneurons and identified one molecule, reelin, as a strong candidate for being a useful marker. Reelin was expressed in the pre-BötC and in more caudal inspiratory bulbospinal ventral respiratory group (ibsVRG) premotoneurons, which were clearly distinguishable by differences in their somatic diameters.

We then studied adult mice lacking the reelin protein (Reeler) to screen for respiratory deficits. These mice exhibited abnormal responses to hypoxia, suggesting that reelin may have a functional postdevelopmental role in breathing.

MATERIALS AND METHODS

Medullary slice preparation

All experiments on animals were carried out with the approval of the UCLA Institutional Animal Care and Use Committee. The preparation of a medullary slice that retains functional respiratory networks and generates respiratory rhythm has been described previously (Smith et al., 1991). Briefly, C57Bl6 neonatal mice of either sex aged P1–P5 were anesthetized, and the brainstem was isolated with care to preserve the XII nerve roots, followed by removal of the cerebellum. The brainstem was pinned down on a paraffin-coated block with the ventral surface upward, and the block was mounted in a Vibratome (VT1000S; Technical Products International, St. Louis, MO). The brainstem was sectioned (slice thickness 500–600 μm) serially in the transverse plane starting from the rostral medulla to the rostral boundary of the pre-BötC. One transverse slice, in which XII was included, was transferred to a recording chamber. The slice was perfused in an artificial cerebrospinal fluid (ACSF) containing (in mM) 128 NaCl, 3.0 KCl, 1.5 $CaCl_2$, 1.0 $MgSO_4$, 23.5 $NaHCO_3$, 0.5 NaH_2PO_4, and 30 glucose, with increased KCl (9 mM) to stimulate the spontaneous rhythmic respiratory motor discharge.

Electrophysiological recording and intracellular mRNA aspiration

Respiratory-related nerve activity was recorded from XII nerve roots with a suction electrode. Patch electrodes were pulled from thick-wall borosilicate glass with a tip size of 1–1.5 μm (resistance 4–6.5 MΩ). The electrode filling solution was prepared with DEPC-treated water and contained (in mM) 140 potassium gluconate, 5.0 NaCl, 0.1 $CaCl_2$, 1.1 EGTA, 2.0 ATP (Mg^{2+} salt), and 1 U/μl RNasin (Ambion, Austin, TX). The whole-cell patch recordings were obtained from the inspiratory neurons that fired in phase with the inspiratory burst from the XII nerve and localized ventrolaterally to the nucleus ambiguous. The intracellular components of inspiratory neurons were carefully aspirated into the tip of

electrode pipette via gently applying a suitable negative pressure under Gigaohm seal condition and were visualized with infrared-differential interference contrast (IR-DIC) microscopy (×400, Axioskop; Carl Zeiss, Heidenheim, Germany). The mRNAs obtained from nucleus ambiguous neurons in the same way as described above were used to synthesize the control cDNAs for subtractive hybridization.

cDNA amplification and single-cell subtractive library construction

Single-cell cDNA amplification was based on methods previously reported (Tietjen et al., 2003). Briefly, the glass pipette tips were immediately broken in 4 μl of ice-cold cell lysis buffer (in mM: 50 Tris-HCl, pH 8.3, 75 KCl, 3 $MgCl_2$, 0.5% NP-40) containing 80 ng/ml oligo-d(T) 12– 16 (Promega, Madison, WI), 1 U/μl RNasin (Ambion, Austin, TX), and 10 μM each of dATP, dCTP, dGTP, and dTTP (Promega, Madison, WI). The lysis buffer with pipette tips was incubated at 65°C for 1 min, followed by addition of 10 U transcriptase (Qiagen, Valencia, CA) and incubation at 37°C for 30 min. The samples were heated at 65°C for 10 min. Poly(A) was tailed to the first-strand cDNA product by adding 4 μl of tailing solution containing 10 U terminal transferase (Promega, Madison, WI), 200 mM potassium cacodylate (pH 7.2), 4 mM $CoCl_2$, 0.4 mM DTT, and 200 μM dATP at 37°C for 15 min. Samples were heat inactivated again at 65°C for 10 min.

The cDNAs were amplified by a specific anchor primer (5′-TTTTTTTTTTTTTTT-3′) via PCR. PCR was carried out using 0.5 U Pfx and 0.25 U Taq (Invitrogen, Carlsbad, CA) DNA polymerase. Biotin-dCTP was incorporated into PCR during the amplification of cDNAs from ambiguous neurons. The cDNA fragments were used to construct a subtractive library after removal of those of length less than 500 base pairs and subtraction from ambiguous neuronal cDNAs. The remaining cDNAs were used to construct a cDNA library using SMART cDNA library construction kit based on the manufacturer's instruction (Clontech, Mountain View, CA). About 3,500 individual colonies were obtained, and most of them contained inspiratory neuronal cDNA fragments of over 500 base pairs (data not shown). The second round of hybridization was performed using biotin-labeled ambiguous neuron cDNAs prepared as described above as probes to decrease the background further. The negative clones were picked up and identified by sequencing.

Immunohistochemistry and antibody characterization

The expression patterns of the candidates (Table 1) in the pre-BötC area were confirmed by immunohistochemistry in adult male Sprague Dawley rats, when an antibody was available, or in situ hybridization in adult mouse brainstem. Table 2 provides a list of all antibodies used in the present study.

The rabbit polyclonal NK1R antibody was raised in rabbit using a synthetic peptide corresponding to the 393–407- amino-acid sequence of NK1R. The antiserum recognizes the NK1R in rat, mouse, and guinea pig (technical information provided by Advanced Targeting Systems, San Diego, CA). The specificity of the antibody has been previously demonstrated (Vigna et al., 1994); the antibody labeled exclusively rat kidney epithelial cells, neurons in the dorsal horn of the spinal cord in the regions corresponding to SP inputs (substantia gelatinosa), and neurons and muscle cells in the ileum; Western blot analysis of proteins obtained from rat kidney epithelial cells that expressed functional NK1Rs showed a broad immunoreactive band corresponding to the NK1R (70 to over 150 kDa). The specificity of the antibody has been further confirmed by demonstrating that it colabels exclusively neurons that have internalized fluorescent SP and thus express the NK1R (Pagliardini et al., 2005). Labeling with this antibody was abolished following preadsorption of diluted antiserum with the immunogenic amino acid sequence (NK1R393- 407; Vigna et al., 1994)

and by lack of staining in tissue in which neurons expressing the NK1R were killed using saporin- conjugated SP (Mantyh et al., 1997).

The goat polyclonal choline acetyltransferase (ChAT) antibody was prepared against the human placental enzyme. In an immunoblot in mouse NIH/3T3 cell lysates, a single band of the correct molecular weight was identified (manufacturer's technical information). In the brainstem, it stains a pattern that is consistent with previous reports (Pagliardini et al., 2011).

The rabbit polyclonal somatostatin (Sst) antibody was prepared against the first 14 aa of the synthetic peptide Sst. The antibody is specific for Sst; no cross-reactivity of the antibody with other peptides such as SP, amylin, glucagon, insulin, neuropeptide Y (NPY), or vasoactive intestinal peptide has been reported from immunoblotting according to the manufacturer's instructions.

The mouse monoclonal reelin antibody (IgG1, clone G10) was prepared against the recombinant reelin residues 164–496 derived from mouse E15–E17 embryonic brain (Yip et al., 2009). On immunoblots from mouse and rat brain lysates, it recognizes a band representing the reelin peptide at ~388 kDa; it stains the Cajal-Retzius cell layer in the marginal zone in embryonic cerebral cortex at 15 days in utero (manufacturer's technical information).

The chicken polyclonal TH antibody (F1005; Aves Labs, Tigard, OR) was prepared against residues 37–50 (RRQ SLI EDA RKE RE) and against residues 439–454 (SDA KDK LR[N/S] YAS RIQ R) of the human gene product (P07101; NCBI). In the second peptide, there was a mixture of asparagine and serine at position 9 to ensure that the antibodies would recognize both human (serine) and mouse (asparagine) gene products. Immunostaining with this antibody yields staining in the brainstem identical to that with the mouse monoclonal antiserum TH (Tan et al., 2008; Millipore, Bedford, MA; MAB5280) in our antibody characterization experiments (data not shown).

For all secondary antibody immunohistochemical controls, the primary antibodies were omitted, and the tissue showed no immunoreactivity above background.

The procedures for immunohistochemistry were described previously (Tan et al., 2008). Rats were anesthetized with Nembutal (100 mg kg^{-1}, i.p.; Lundbeck Inc., Deerfield, IL) and perfused transcardially with 4% paraformadehyde in phosphate-buffered saline (PBS; 137 mM NaCl, 2.7 mM KCl, 8.1 mM $Na_2HPO_4{\cdot}2H_2O$, 1.76 mM KH_2PO_4, pH7.4). The brainstem was removed and postfixed in 4% paraformadehyde/PBS overnight at 4°C, followed by cryoprotection overnight in 30% sucrose in PBS. Forty-micrometer-thick transverse or sagittal sections were cut using a cryostat and incubated in the primary antibodies described above, with 10% normal donkey serum for 24 or 48 hours at 4°C. After a series of washes, the primary antibodies were detected by using the specific secondary antibodies (dilution 1:250): rhodamine-conjugated donkey anti-rabbit and rhodamine-conjugated donkey anti-chicken (Jackson Immunoresearch, West Grove, PA) and Alexa 488-conjugated donkey anti-mouse secondary antibodies (Invitrogen, Calsbad, CA). Sections were then washed, mounted on gelatin-coated slides, and coverslipped.

For reelin DAB staining, the sections were washed in PBS briefly, followed by blocking with 10% donkey serum in PBS with 0.3% triton 100 for 1 hour at room temperature. The primary antibody G10 was incubated with sections overnight at room temperature. The secondary biotinylated donkey anti-mouse (1:1,000; Jackson Immunoresearch) was added to the sections for 2 hours at room temperature after three washes by PBS/Triton 100 solution. The Vectastain ABC reagent (Vector, Burlingame, CA) was added and incubated for 1 hour, and the color was developed using DAB reagent (Vector, Burlingame, CA) after three

washes. The sections were stained brown with DAB only or black by adding 0.05% cobalt chloride and 0.01% nickel' ammonium sulfate to the DAB solution. The tissue was mounted on gelatin-coated slides, dehydrated in graded ethanols, cleared in xylenes, and coverslipped.

Brainstem sections were grouped as one-in-six of sequential series of 40-μm transverse sections; six groups of brainstem sections were collected from each rat, and immunohistochemistry was performed using the following three groups of primary antibodies: Sst/reelin, NK1R/reelin, TH/reelin. Images were acquired by confocal laser scanning microscopy (LSM510 Meta; Carl Zeiss, Heidenheim, Germany). For Alexa 488, excitation (argon, 1 mV) was set to 488 nm, and emissions were gathered with a 500–530-nm bandpass filter. For rhodamine fluorescence, excitation (HeNe, 1 mV) was set to 543 nm, and emissions were gathered with a 560–615-nm bandpass filter. For experiments involving FG, images were taken with an epifluorescence microscope using a mercury arc lamp (Axioplan 2; Carl Zeiss, Heidenheim, Germany). Z-stack images were acquired at ×20 or ×40 magnification, and images were exported to Adobe Illustrator (Adobe, San Jose, CA) for figure composition. The images were cropped into suitable sizes without any other type of modification, such as contrast or brightness. Three different ages of rats, 4 weeks (n = 4), 8 weeks (n = 5), and 24 weeks (n = 4), were used for cellcounting experiments. Briefly, sagittal sections from one hemisphere of brainstem of each rat were obtained and incubated with reelin G10 antibody, followed by the diaminobenzidine (DAB) staining procedure as described above. Sagittal sections containing pre-BötC area (usually three sections) from one hemisphere of the brainstem were set as one group. Mosaic images of whole sagittal sections were acquired by brightfield light microscopy (Axioplan 2; Carl Zeiss, Heidenheim, Germany) using AxioVision software (Carl Zeiss, Heidenheim, Germany). During cell counting, each image of one sagittal section was divided along the rostral–caudal axis into an array of columns running dorsal to ventral with exactly 100 μm spanning width. Each column's position relative to Bregma was determined by its distance to the caudual edge of the VII motor nucleus, e.g., Bregma −11.7 mm based on the rat atlas of Paxinos and Watson. Reelin-positive neurons in the DFG and ventrolateral medulla in every column of the section were counted. The reelin neurons from all columns in the same Bregma level were set as one group, and data are presented as mean ± SD.

In situ hybridization

Male mice aged 6–8 weeks were used for the experiments. The mice were anesthetized by isoflurane and decapitated. The brainstems were rapidly removed and frozen in methybulton in dry ice. Brainstems were stored at −80°C until sectioning. The coronal sections were cut at 12 μm thickness, mounted on gelatin-coated slides, and kept at −80°C until the day of the experiment.

The PCR fragments with 5′ flanking T7 promoter sequence and 3′ flanking T3 promoter sequence were used to synthesize ^{35}S-radiolabeled RNA probes. The RNA probes were transcribed following standard protocols (Chesselet and Affolter, 1987). Briefly, 400 ng of PCR fragments was used for 20 μl synthesis mixture containing 10 μM UTP; 2.5 μM ^{35}S-UTP (1,000 Ci/mmol); 10 μM each of ATP, CTP, and GTP; 5 mM of dithiothreitol; 20 U superRNAsin (Ambion, Austin, TX); and 10 U T7 or T3 RNA polymerase (Promega, Madison, WI). The probes were extracted in phenol/ chloroform/isoamyl alcohol and precipitated overnight in ethanol at −80°C. All the solutions and buffers were prepared with 0.1% diethylpyrocarbonate (DEPC)-treated distilled water. Sections were removed from −80°C and completely dried on dry ice under a stream of cool air. Sections were postfixed by 3% paraformaldehyde containing 0.02% DEPC, acetylated, and dehydrated. Then, 3–6 ng of probe (4 million dpm/ng) in hybridization mixture was applied to each section. Hybridizations were carried out at 50°C for 12–14 hours in humid chambers.

Posthybridization washes included three times in 50% formamide in 2× SSC (0.3 M NaCl/0.03 M sodium citrate) at 52°C for 30 min, followed by a 30-min incubation of RNase A (100 μg /ml; Promega, Madison, WI) at 37°C and an overnight rinse in 2× SSC with 0.05% Triton X-100. The sections were then dehydrated through graded ethanols and xylenes and dried in the air. The sections were first exposed to BioMax X-film (Kodak, Rochester, NY) for 1 week and subsequently dipped into Kodak NTB3 emulsion (Kodak, Rochester, NY) and exposed for 10–30 days. Sections were developed in D19 (3.5 minutes) fixed in Kodak fixative (5 minutes), counterstained by hemotoxylin-eosin, and mounted with Eukitt (Electron Microscopy Sciences, Hatfield, PA). The sections were examined under light- and darkfield microscopy.

Plethysmograph recording and data analysis

Reeler mice and their littermates were kindly provided by Prof. P. Phelps of the University of California, Los Angeles. Adult male mice aged 6–8 weeks were recorded using a whole-body mouse plethysmograph (Buxco Research Systems, Sharon, CT). The signal from the plethysmograph corresponds to changes in tidal volume. While in the plethysmograph, the mouse could move freely, with access to water and chow. Reeler mice and their littermates were studied for 4 hours in the plethysmograph. For hypoxia and hypercapnia challenges, the mice were challenged for 5 min with 8% O_2 or 5% CO_2, respectively, and data were collected from the final 30 seconds of the challenge.

Surgical procedure for tracing bulbospinal neurons

For spinal injections under ketamine anesthesia (50 mg/kg, Ketaject; Phoenix Pharmaceuticals, St. Joseph, MO), a hole was drilled into the C4 vertebrae and a fine glass pipette containing FG (5%; Fluorochrome, Denver, CO) was lowered into the ventral horn based on the rat atlas of Paxinos and Watson. A 100-nl solution containing the tracer was injected by an air pressure system. After 5 additional minutes, the pipette was slowly withdrawn, and the incision was sutured with absorbable sutures for inner muscles and nonabsorbable nylon sutures for the skin. Animals survived for 7 days.

RESULTS

Construction and screening of a pre-BötC inspiratory neuron subtractive cDNA library

The pre-BötC contains respiratory-related neurons with several distinct activity patterns, including inspiratory and expiratory (Guyenet and Wang, 2001; Schwarzacher et al., 1995). Individual pre-BötC neurons from neonatal mice were whole-cell patched from the rostral slice surface (Fig. 1A,C), and hypoglossal nerve activity was measured via a suction electrode (Fig. 1A,B). The intraneuronal components of pre-BötC inspiratory neurons (n = 12) and of nucleus ambiguous (NA) motoneurons (n = 10) were aspirated into patch electrodes (Fig. 1B,C) and processed to construct a subtractive cDNA library (see Materials and Methods). Forty-nine candidate genes with greatly enhanced expression in the pre-BötC compared with NA were obtained. Twelve of these candidates were expressed sequence tags (ESTs) belonging to unknown genes (data not shown); the rest were known or predicted genes that belong to several categories, including kinases, GTPases, transcriptional factors, Ca^{2+}-binding proteins, membrane proteins, and cytoskeleton-related proteins (Table 1).

Expression patterns of candidate genes in pre-BötC

The expression patterns of adult rat pre-BötC gene candidates were confirmed by immunohistochemistry when an antibody was available or by in situ hybridization (in adult mice). Some candidates did not show detectable expression levels in the brainstem (data not shown) by either technique. Some other candidates showed ubiquitous expression

throughout the brainstem in adult mice, e.g., visinin-like 1, a calcium sensor protein (data not shown), whereas others exhibited high levels of expression restricted to various brainstem nuclei including the pre-BötC in adult mice. 1) The progesterone receptor membrane component 1 (PRMC1) gene was highly expressed in the vestibular nucleus, solitary tract, and inferior olive, with more moderate expression in the pre-BötC (Fig. 2, top). The presence of PRMC1 in the pre-BötC indicates that some hormones may directly modulate breathing. 2) The Abelson helper integration site (Ahi1) gene was highly expressed in the vestibular nucleus and solitary tract and at moderate levels in the pre-BötC (Fig. 2, middle). Mutations in Ahi1 cause Joubert syndrome, an autosomal recessive disorder with hypotonia, ataxia, developmental delay, oculomotor apraxia, and neonatal breathing abnormalities (Dixon-Salazar et al., 2004; Ferland et al., 2004). The expression of Ahi1 in pre- BötC may underlie these breathing abnormalities. 3) Latexin, an endogenous carboxypeptidase inhibitor, was expressed in the hypoglossal, facial, ambiguus nuclei, and Bötzinger complex (BötC), with a few scattered neurons in the rostral pre-BötC (Fig. 2, bottom). 4) A novel exon of cAMP-dependent protein kinase inhibitor (PKI) gamma was also expressed in the pre-BötC. This 158-bp exon was the first exon and separated by 44-kbp intron 1 from exon 2 (data not shown). Here, we focus on reelin, which was highly expressed in a subset of pre-BötC neurons but in few other structures in the brainstem.

Reelin expression profile in the rat brainstem—*Reelin* is a secreted glycoprotein that plays an important role in corticogenesis and neuronal positioning during their development (D'Arcangelo, 2001; D'Arcangelo et al., 1995; Miao et al., 1994; Molnar et al., 1998). In the medulla, *reelin* neurons were located in adult rats in four regions related to brainstem control of breathing (Fig. 3): i) preBötC extending caudally into the ibsVRG; ii) a diffuse area dorsal to the facial nucleus which we designate as the dorsal facial group (DFG); iii) a region containing premotoneurons projecting to hypoglossal motoneurons which we designate as the parahypoglossal group (PHG) (Tan et al., 2010), and; iv) pontine respiratory group

The reelin antibody labeled neuronal somata but not processes in the brainstem. Reelin neurons were concentrated below the caudal NA compact division and about 500 μm from the caudal edge of the facial nucleus (Bregma −11.7 mm) in the ventrolateral medulla, i.e., pre- BötC (Fig. 3A–C). Reelin neurons extended more caudally from pre-BötC to the rostral VRG, which contains bulbospinal inspiratory premotor neurons. NA motoneurons did not show any expression of reelin, which is expected from results of the subtractive hybridization using cDNAs from NA single cell as control. There were a few reelin-expressing neurons in the BötC between Bregma levels −11.8 and −12.3 mm (Figs. 3A, 5A). The number of reelin neurons gradually increased along the rostral-caudal axis in the ventrolateral medulla between Bregma levels −11.8 to −12.8 mm. The peak distribution of reelin neurons in the ventrolateral medulla was between Bregma levels −12.8 and −13.0 mm, 1.1 mm from the caudal edge of the facial nucleus (Bregma −11.7 mm), after which the number of reelin neurons decreased along the longitude axis of the ventrolateral medulla (Fig. 5A). Ninety percent of reelin neurons were concentrated between Bregma levels −12.3 and −13.6 mm. The number of reelin neurons in the pre- BötC and VRG decreased slightly in 24-week-old rats in comparison with 2- and 8-week-old rats (Fig. 5A).

NK1R and Sst immunoreactivities define subpopulations of pre-BötC neurons (Gray et al., 1999, 2001; Stornetta et al., 2003). We next investigated whether these two molecules were coexpressed in reelin neurons. In the ventrolateral medulla, the majority of NK1R (84.0% ±7.4%, n = 4; Fig. 4A–C) and Sst neurons (84.9% ±6.1%, n = 4; Fig. 4D–F) coexpressed reelin, but not the converse. This result suggests that reelin neurons encompass a larger population of pre-BötC neurons than NK1R and Sst neurons. There was no overlap between

TH neurons and reelin neurons (Fig. 4G,H), showing that these neurons are not catecholaminergic.

Reelin neurons were also found in the parahypoglossal group (PHG; Fig. 3D), a region innervated by pre-BötC neurons (Tan et al., 2010) that is thought to contain hypoglossal premotor neurons. The expression of reelin in PHG neurons was highest in young rats (~8 weeks old), but it was barely detectable in older rats (24 weeks old; data not shown).

Reelin neurons were found in a diffuse area dorsal to the facial nucleus, which we refer to as *DFG* (Fig. 3E). These reelin neurons were concentrated in an area ~200–300 μm above the dorsal boundary of the facial nucleus (RC 1.1 mm, DV 0.6 mm, ML 0.5 mm), between Bregma levels −10.4 and −11.7 mm. More rostrally, we observed a band of reelin neurons that extended in sagittal sections from the dorsal boundary of the trigeminal nucleus dorsally and rostrally to the caudal boundary of the pedunculopontine tegmentum (PPT; Fig. 3F). This band includes portions of the supratrigeminal nucleus, medial and lateral parabrachial nuclei, and Kölliker-Fuse, which comprise the pontine respiratory group (PRG). In addition to these respiratory areas, reelin neurons were found in the ventromedial medulla, an area containing many glutamatergic and GABAergic bulbospinal premotoneurons.

Difference in soma size distinguishes pre-BötC from ibsVRG reelin neurons

Although there was a continuous column of reelin neurons extending caudally from the pre-BötC, we observed two distinct populations based on soma size, transitioning at Bregma level −12.8 mm, with the population with smaller somata more rostral. We hypothesized that the anatomic boundary between these populations was at the caudal pre-BötC border, with the more caudal population being the ibsVRG. To test this hypothesis, we injected the retrograde tracer FG into the C2–C4 spinal cord ventral horn. Seven days after injection, FG strongly labeled neurons in the VRG, defining a population of bulbospinal neurons caudal to the pre-BötC. Immunolabeling for reelin colabeled FG-positive neurons with an average soma diameter of 26.5 6 3.7 μm based on immunofluorescent staining (n = 30) and of 27.1 ± 3.8 μm based on DAB staining (n = 135; Fig. 5B). The more rostral pre-BötC reelin neurons (Fig. 5C–G) had significantly smaller soma diameters based on DAB staining of 15.5 ± 2.4 μm (n = 130; $P = 0.00002$).

Impaired response to respiratory challenges suggests a respiratory role for reelin in mouse

We examined whether the loss of reelin had any functional consequences for respiration. We chose to study Reeler (Falconer, 1951) transgenic mice, which lack functional reelin protein, as a broad screen of respiratory involvement of the reelin protein.

Reeler mice exhibited an impaired response to hypoxia, but responded to hypercapnea. Awake in room air at rest, fI of Reeler mice was 154.7 ± 4.8 breaths/min and of their (control) littermates was 162.7 ± 5.1 breaths/min ($n = 5$; $p = 0.03$) (Fig. 6). In response to hypercapnea (5% CO_2 −21% O_2−74% N_2), f_I in both groups of mice increased similarly: Reeler mice to 245.9 ± 45.0 breaths/min ($n = 5$; $p = 0.002$) and control mice to 269.7 ± 18.3 breaths/ min ($n = 5$; p ¼1.5 × 10^{-6}) (Fig. 6); there was no difference between the groups ($p = 0.31$). In response to hypoxia (8% O_2–92%N_2), f_I did not change in Reeler mice (148.5 6 23.6 breaths/min; $n = 5$; $p = 0.50$), whereas control mice had the classic robust increase (235.3 6 25.5 breaths/min; $p = 0.0002$) (Fig. 6).

DISCUSSION

When studying a heterogeneous population of neurons, such as those making up the pre-BötC, defining cell types according to their activity and gene and protein expression profiles

are of considerable utility. Here we constructed a cDNA library for screening candidate genes from pre-BötC inspiratory neurons. To obtain genetic material from these neurons, we whole-cell patched them and extracted the mRNA through the patch pipette. This ensured the purity of the genetic material, without contamination from neighboring cells or processes connecting to the neuron. Because mRNA obtained via patch electrode may represent only a portion of the total cellular mRNA of any neuron and because our goal was to identify candidate genes that we would subsequently verify with other techniques, we combined the extracted contents from 12 pre-BötC inspiratory neurons during the subtractive hybridization procedure. At this point, we did not differentiate between inspiratory-modulated glutamatergic and glycinergic neurons. We used exponential amplification to multiply the cDNAs. We obtained efficient amplification for the 3′ portion of highly expressed genes from pre-BötC inspiratory neurons by using a single poly (dT)-tailed primer after tagging 3′ ends of cDNAs with poly(dA). With this strategy, we successfully constructed a subtractive cDNA library from pre- BötC inspiratory neurons compared with NA motoneurons and obtained several molecular candidates (see Results). We focused on reelin, which was highly expressed in pre- BötC neurons and neighboring ibsVRG neurons and relatively few other areas in the brainstem.

We found that reelin demarcates a subset of pre-BötC neurons that may set the caudal boundary between the pre-BötC and ibsVRG. Reelin is a secreted extracellular glycoprotein essential in prenatal development for neuronal migration and positioning (Alcantara et al., 1998; Cooper, 2008; D'Arcangelo et al., 1995; Rice and Curran, 2001; Soriano and Del Rio, 2005). Reelin is also implicated in the modulation of synaptic plasticity, stimulation of synaptic terminal density and hypertrophy of dendritic spines, and enhancement of glutamate-evoked Ca^{2+} currents via NMDA receptor subunits in adult animals (Alcantara et al., 2006; Beffert et al., 2005; Groc et al., 2007; Herz and Chen, 2006; Niu et al., 2008; Pesold et al., 1998, 1999; Pujadas et al., 2010).

The expression level of reelin is altered in some neurological diseases, such as schizophrenia (Guidotti et al., 2000; Herz and Chen, 2006; Impagnatiello et al., 1998; Knable et al., 2001), psychotic bipolar disorder (Guidotti et al., 2000; Veldic et al., 2007), and Alzheimer's disease (Botella-Lopez et al., 2006; Seripa et al., 2008). Two members of the low-density lipoprotein receptor gene family mediate the reelin signaling pathway: apolipoprotein E receptor 2 (ApoER2) and very-low-density lipoprotein receptor (VLDLR; Herz and Chen, 2006). Many molecules are involved in the signaling cascade triggered by reelin, including SFK, Dab1, Lis1, and PI3K (Herz and Chen, 2006).

Reelin expression partially overlaps with two known markers for glutamatergic pre-BötC neurons: somatostatin and NK1 receptor. The extent of heterogeneity among pre-BötC neurons is currently unknown, and the distinction between neurons that express one, two, or all three of these markers is unclear. At present, we are unable to determine whether all pre-BötC reelin neurons are involved in the neural control of breathing. However, strong colocalization with two other pre-BötC markers suggests that many of these neurons are critical to breathing.

The PHG receives projections from pre-BötC Sst neurons (Tan et al., 2010). We hypothesize that this region contains premotor neurons to hypoglossal motoneurons and interneurons relaying signals from the pre-BötC to nucleus of the solitary tract (nTS). Interestingly, there were many reelin neurons in this region in young rats, but this reelin expression in PHG dramatically decreased in older rats. The reason for this age-related change in reelin expression and the function of reelin neurons in the PHG are presently unknown. We also found a group of reelin neurons residing dorsal to the facial nucleus that maintained reelin

expression across age groups. Their anatomical connections and function, respiratory or otherwise, are also currently unidentified.

We found substantial numbers of reelin neurons in the PRG, forming a band from the trigeminal motor nucleus sweeping dorsally and rostrally to the pedunculopontine tegmentum. This group of neurons included portions of the supratrigeminal nucleus, medial and lateral parabrachial nuclei, and Kölliker-Fuse. The role of these reelin neurons is currently unknown, although these areas contain many respiratory-phased neurons with projections to medullary respiratory targets. In addition, this area receives dense projections from Sst pre-BötC neurons (Tan et al., 2010).

Most of the areas containing reelin neurons outside of the pre-BötC are known or presumed to contain premotor neurons. The only nonrespiratory area with identified reelin neurons was in the ventromedial medulla, which is also a site of nonrespiratory bulbospinal premotor neurons (Lai and Siegel, 1988; Vetrivelan et al., 2009).

The Reeler mouse was first described in 1951 (Falconer, 1951), and later the locus of the *reelin* gene was mapped and identified (D'Arcangelo et al., 1995; Miao et al., 1994). Reeler mice have characteristic "reeling" movements and show many pathological brain structures, including inversion of cortical layers (Molnar et al., 1998), decreased cerebellar size (Hamburgh, 1963), and impaired dendrite outgrowth (Niu et al., 2004). We found that Reeler mice had an impaired response to hypoxia compared with their littermates. Although the loss of reelin in these knockouts is complete and thus does not allow us to pinpoint the origin of any breathing deficit, these results are suggestive of a role for reelin in 1) the development of circuits that modulate breathing in response to hypoxia or 2) mediating the hypoxic response in adults rats. It is also worth noting that Reeler mice having a normal response to hypercapneic challenge is consistent with the absence of reelin labeling found within the RTN/pFRG as well as other chemosensitive areas. The pre-BötC is hypothesized to be a site sensitive to hypoxia (Solomon et al., 2000). If this were the case, then a possible consequence of the absence of reelin would be to diminish the hypoxic response in mutants while leaving the hypercapnic response intact. However, because the reelin mutation affects sites other than the pre-BötC, this possibility remains speculative pending further and more specific testing.

In summary, we successfully constructed a subtractive cDNA library from pre-BötC inspiratory neurons and determined that reelin clearly labels a subset. The anatomical boundary of the pre-BötC and ibsVRG is at the border of two reelin populations with distinct soma diameters. Mice lacking functional reelin protein exhibited abnormal responses to hypoxia, indicating a possible modulatory role for reelin in breathing in the adult.

Supplementary Material

Refer to Web version on PubMed Central for supplementary material.

Acknowledgments

Grant sponsor: National Institutes of Health; Grant number: HL40959.

The authors thank Dr. Marie-Francoise Chesselet at UCLA for providing technical support for in situ hybridization and Dr. Patricia Phelps at UCLA for providing the Reeler mice. We also thank Grace Li for experimental assistance.

LITERATURE CITED

Alcantara S, Ruiz M, D'Arcangelo G, Ezan F, de Lecea L, Curran T, Sotelo C, Soriano E. Regional and cellular patterns of reelin mRNA expression in the forebrain of the developing and adult mouse. J Neurosci. 1998; 18:7779–7799. [PubMed: 9742148]

Alcantara S, Pozas E, Ibanez CF, Soriano E. BDNF-modulated spatial organization of Cajal-Retzius and GABAergic neurons in the marginal zone plays a role in the development of cortical organization. Cereb Cortex. 2006; 16:487–499. [PubMed: 16000651]

Beffert U, Weeber EJ, Durudas A, Qiu S, Masiulis I, Sweatt JD, Li WP, Adelmann G, Frotscher M, Hammer RE, Herz J. Modulation of synaptic plasticity and memory by Reelin involves differential splicing of the lipoprotein receptor Apoer2. Neuron. 2005; 47:567–579. [PubMed: 16102539]

Bianchi AL, Denavit-Saubie M, Champagnat J. Central control of breathing in mammals: neuronal circuitry, membrane properties, and neurotransmitters. Physiol Rev. 1995; 75:1–45. [PubMed: 7831394]

Botella-Lopez A, Burgaya F, Gavin R, Garcia-Ayllon MS, Gomez-Tortosa E, Pena-Casanova J, Urena JM, Del Rio JA, Blesa R, Soriano E, Saez-Valero J. Reelin expression and glycosylation patterns are altered in Alzheimer's disease. Proc Natl Acad Sci U S A. 2006; 103:5573–5578. [PubMed: 16567613]

Bouvier J, Thoby-Brisson M, Renier N, Dubreuil V, Ericson J, Champagnat J, Pierani A, Chedotal A, Fortin G. Hindbrain interneurons and axon guidance signaling critical for breathing. Nat Neurosci. 2010; 13:1066–1074. [PubMed: 20680010]

Chan RK, Sawchenko PE. Organization and transmitter specificity of medullary neurons activated by sustained hypertension: implications for understanding baroreceptor reflex circuitry. J Neurosci. 1998; 18:371–387. [PubMed: 9412514]

Chesselet MF, Affolter HU. Preprotachykinin messenger RNA detected by in situ hybridization in striatal neurons of the human brain. Brain Res. 1987; 410:83–88. [PubMed: 3580901]

Cooper JA. A mechanism for inside-out lamination in the neocortex. Trends Neurosci. 2008; 31:113–119. [PubMed: 18255163]

D'Arcangelo G. The role of the reelin pathway in cortical development. Symp Soc Exp Biol. 2001; 53:59–73. [PubMed: 12063849]

D'Arcangelo G, Miao GG, Chen SC, Soares HD, Morgan JI, Curran T. A protein related to extracellular matrix proteins deleted in the mouse mutant reeler. Nature. 1995; 374:719–723. [PubMed: 7715726]

Dixon-Salazar T, Silhavy JL, Marsh SE, Louie CM, Scott LC, Gururaj A, Al-Gazali L, Al-Tawari AA, Kayserili H, Sztriha L, Gleeson JG. Mutations in the AHI1 gene, encoding jouberin, cause Joubert syndrome with cortical polymicrogyria. Am J Hum Genet. 2004; 75:979–987. [PubMed: 15467982]

Falconer DS. Two new mutants, "Trembler" and "Reeler," with neurological actions in the house mouse (Mus musculus L.). J Genet. 1951; 50:192–205.

Ferland RJ, Eyaid W, Collura RV, Tully LD, Hill RS, Al-Nouri D, Al-Rumayyan A, Topcu M, Gascon G, Bodell A, Shugart YY, Ruvolo M, Walsh CA. Abnormal cerebellar development and axonal decussation due to mutations in AHI1 in Joubert syndrome. Nat Genet. 2004; 36:1008–1013. [PubMed: 15322546]

Gray PA, Rekling JC, Bocchiaro CM, Feldman JL. Modulation of respiratory frequency by peptidergic input to rhythmogenic neurons in the pre-Botzinger complex. Science. 1999; 286:1566–1568. [PubMed: 10567264]

Gray PA, Janczewski WA, Mellen N, McCrimmon DR, Feldman JL. Normal breathing requires pre-Botzinger complex neurokinin-1 receptor-expressing neurons. Nat Neurosci. 2001; 4:927–930. [PubMed: 11528424]

Gray PA, Hayes JA, Ling GY, Llona I, Tupal S, Picardo MC, Ross SE, Hirata T, Corbin JG, Eugenin J, Del Negro CA. Developmental origin of pre-Botzinger complex respiratory neurons. J Neurosci. 2010; 30:14883–14895. [PubMed: 21048147]

Groc L, Choquet D, Stephenson FA, Verrier D, Manzoni OJ, Chavis P. NMDA receptor surface trafficking and synaptic subunit composition are developmentally regulated by the extracellular matrix protein reelin. J Neurosci. 2007; 27:10165–10175. [PubMed: 17881522]

Guidotti A, Auta J, Davis JM, Di-Giorgi-Gerevini V, Dwivedi Y, Grayson DR, Impagnatiello F, Pandey G, Pesold C, Sharma R, Uzunov D, Costa E. Decrease in reelin and glutamic acid decarboxylase 67 (GAD67) expression in schizophrenia and bipolar disorder: a postmortem brain study. Arch Gen Psychiatry. 2000; 57:1061–1069. [PubMed: 11074872]

Guyenet PG. Neural structures that mediate sympathoexcitation during hypoxia. Respir Physiol. 2000; 121:147–162. [PubMed: 10963771]

Guyenet PG, Wang H. Pre-Botzinger neurons with preinspiratory discharges “in vivo” express NK1 receptors in the rat. J Neurophysiol. 2001; 86:438–446. [PubMed: 11431523]

Hamburgh M. Analysis of the postnatal developmental effects of “reeler,” a neurological mutation in mice A study in developmental genetics. Dev Biol. 1963; 19:165–185. [PubMed: 14069672]

Hayashi M, Yamashita A, Shimizu K. Somatostatin and brain-derived neurotrophic factor mRNA expression in the primate brain: decreased levels of mRNAs during aging. Brain Res. 1997; 749:283–289. [PubMed: 9138728]

Herz J, Chen Y. Reelin, lipoprotein receptors and synaptic plasticity. Nat Rev Neurosci. 2006; 7:850–859. [PubMed: 17053810]

Impagnatiello F, Guidotti AR, Pesold C, Dwivedi Y, Caruncho H, Pisu MG, Uzunov DP, Smalheiser NR, Davis JM, Pandey GN, Pappas GD, Tueting P, Sharma RP, Costa E. A decrease of reelin expression as a putative vulnerability factor in schizophrenia. Proc Natl Acad Sci U S A. 1998; 95:15718–15723. [PubMed: 9861036]

Janczewski WA, Feldman JL. Distinct rhythm generators for inspiration and expiration in the juvenile rat. J Physiol. 2006; 570:407–420. [PubMed: 16293645]

Knable MB, Torrey EF, Webster MJ, Bartko JJ. Multivariate analysis of prefrontal cortical data from the Stanley Foundation Neuropathology Consortium. Brain Res Bull. 2001; 55:651–659. [PubMed: 11576762]

Lai Y, Siegel J. Medullary regions mediating atonia. J Neurosci. 1988; 8:4790–4796. [PubMed: 2904495]

Lu T, Pan Y, Kao SY, Li C, Kohane I, Chan J, Yankner BA. Gene regulation and DNA damage in the ageing human brain. Nature. 2004; 429:883–891. [PubMed: 15190254]

Mantyh PW, Rogers SD, Honore P, Allen BJ, Ghilardi JR, Li J, Daughters RS, Lappi DA, Wiley RG, Simone DA. Inhibition of hyperalgesia by ablation of lamina I spinal neurons expressing the substance P receptor [see comments]. Science. 1997; 278:275–279. [PubMed: 9323204]

Miao GG, Smeyne RJ, D’Arcangelo G, Copeland NG, Jenkins NA, Morgan JI, Curran T. Isolation of an allele of reeler by insertional mutagenesis. Proc Natl Acad Sci U S A. 1994; 91:11050–11054. [PubMed: 7972007]

Molnar Z, Adams R, Goffinet AM, Blakemore C. The role of the first postmitotic cortical cells in the development of thalamocortical innervation in the reeler mouse. J Neurosci. 1998; 18:5746–5765. [PubMed: 9671664]

Niu S, Renfro A, Quattrocchi CC, Sheldon M, D’Arcangelo G. Reelin promotes hippocampal dendrite development through the VLDLR/ApoER2-Dab1 pathway. Neuron. 2004; 41:71–84. [PubMed: 14715136]

Niu S, Yabut O, D’Arcangelo G. The Reelin signaling pathway promotes dendritic spine development in hippocampal neurons. J Neurosci. 2008; 28:10339–10348. [PubMed: 18842893]

Pagliardini S, Adachi T, Ren J, Funk GD, Greer JJ. Fluorescent tagging of rhythmically active respiratory neurons within the pre-Botzinger complex of rat medullary slice preparations. J Neurosci. 2005; 25:2591–2596. [PubMed: 15758169]

Pagliardini S, Janczewski WA, Tan W, Dickson CT, Deisseroth K, Feldman JL. Active expiration induced by excitation of ventral medulla in adult anesthetized rats. J Neurosci. 2011; 31:2895–2905. [PubMed: 21414911]

Pesold C, Impagnatiello F, Pisu MG, Uzunov DP, Costa E, Guidotti A, Caruncho HJ. Reelin is preferentially expressed in neurons synthesizing gamma-aminobutyric acid in cortex and hippocampus of adult rats. Proc Natl Acad Sci U S A. 1998; 95:3221–3226. [PubMed: 9501244]

Pesold C, Liu WS, Guidotti A, Costa E, Caruncho HJ. Cortical bitufted, horizontal, and Martinotti cells preferentially express and secrete reelin into perineuronal nets, nonsynaptically modulating gene expression. Proc Natl Acad Sci U S A. 1999; 96:3217–3222. [PubMed: 10077664]

Pujadas L, Gruart A, Bosch C, Delgado L, Teixeira CM, Rossi D, de Lecea L, Martinez A, Delgado-Garcia JM, Soriano E. Reelin regulates postnatal neurogenesis and enhances spine hypertrophy and long-term potentiation. J Neurosci. 2010; 30:4636–4649. [PubMed: 20357114]

Rice DS, Curran T. Role of the reelin signaling pathway in central nervous system development. Annu Rev Neurosci. 2001; 24:1005–1039. [PubMed: 11520926]

Schwarzacher SW, Smith JC, Richter DW. Pre-Botzinger complex in the cat. J Neurophysiol. 1995; 73:1452–1461. [PubMed: 7643160]

Seripa D, Matera MG, Franceschi M, Daniele A, Bizzarro A, Rinaldi M, Panza F, Fazio VM, Gravina C, D'Onofrio G, Solfrizzi V, Masullo C, Pilotto A. The RELN locus in Alzheimer's disease. J Alzheimers Dis. 2008; 14:335–344. [PubMed: 18599960]

Smith JC, Ellenberger HH, Ballanyi K, Richter DW, Feldman JL. Pre-Botzinger complex: a brainstem region that may generate respiratory rhythm in mammals. Science. 1991; 254:726–729. [PubMed: 1683005]

Solomon IC, Edelman NH, Neubauer JA. Pre-Botzinger complex functions as a central hypoxia chemosensor for respiration in vivo. J Neurophysiol. 2000; 83:2854–2868. [PubMed: 10805683]

Soriano E, Del Rio JA. The cells of Cajal-Retzius: still a mystery one century after. Neuron. 2005; 46:389–394. [PubMed: 15882637]

Standish A, Enquist LW, Schwaber JS. Innervation of the heart and its central medullary origin defined by viral tracing. Science. 1994; 263:232–234. [PubMed: 8284675]

Stornetta RL, Rosin DL, Wang H, Sevigny CP, Weston MC, Guyenet PG. A group of glutamatergic interneurons expressing high levels of both neurokinin-1 receptors and somatostatin identifies the region of the pre-Bötzinger complex. J Comp Neurol. 2003; 455:499–512. [PubMed: 12508323]

Tan W, Janczewski WA, Yang P, Shao XM, Callaway EM, Feldman JL. Silencing preBotzinger complex somatostatin-expressing neurons induces persistent apnea in awake rat. Nat Neurosci. 2008; 11:538–540. [PubMed: 18391943]

Tan W, Pagliardini S, Yang P, Janczewski WA, Feldman JL. Projections of pre-Botzinger complex neurons in adult rats. J Comp Neurol. 2010; 518:1862–1878. [PubMed: 20235095]

Tietjen I, Rihel JM, Cao Y, Koentges G, Zakhary L, Dulac C. Single-cell transcriptional analysis of neuronal progenitors. Neuron. 2003; 38:161–175. [PubMed: 12718852]

Veldic M, Kadriu B, Maloku E, Agis-Balboa RC, Guidotti A, Davis JM, Costa E. Epigenetic mechanisms expressed in basal ganglia GABAergic neurons differentiate schizophrenia from bipolar disorder. Schizophr Res. 2007; 91:51–61. [PubMed: 17270400]

Vetrivelan R, Fuller PM, Tong Q, Lu J. Medullary circuitry regulating rapid eye movement sleep and motor atonia. J Neurosci. 2009; 29:9361–9369. [PubMed: 19625526]

Vigna SR, Bowden JJ, McDonald DM, Fisher J, Okamoto A, McVey DC, Payan DG, Bunnett NW. Characterization of antibodies to the rat substance P (NK-1) receptor and to a chimeric substance P receptor expressed in mammalian cells. J Neurosci. 1994; 14:834–845. [PubMed: 7507985]

Yip YP, Mehta N, Magdaleno S, Curran T, Yip JW. Ectopic expression of reelin alters migration of sympathetic preganglionic neurons in the spinal cord. J Comp Neurol. 2009; 515:260–268. [PubMed: 19412957]

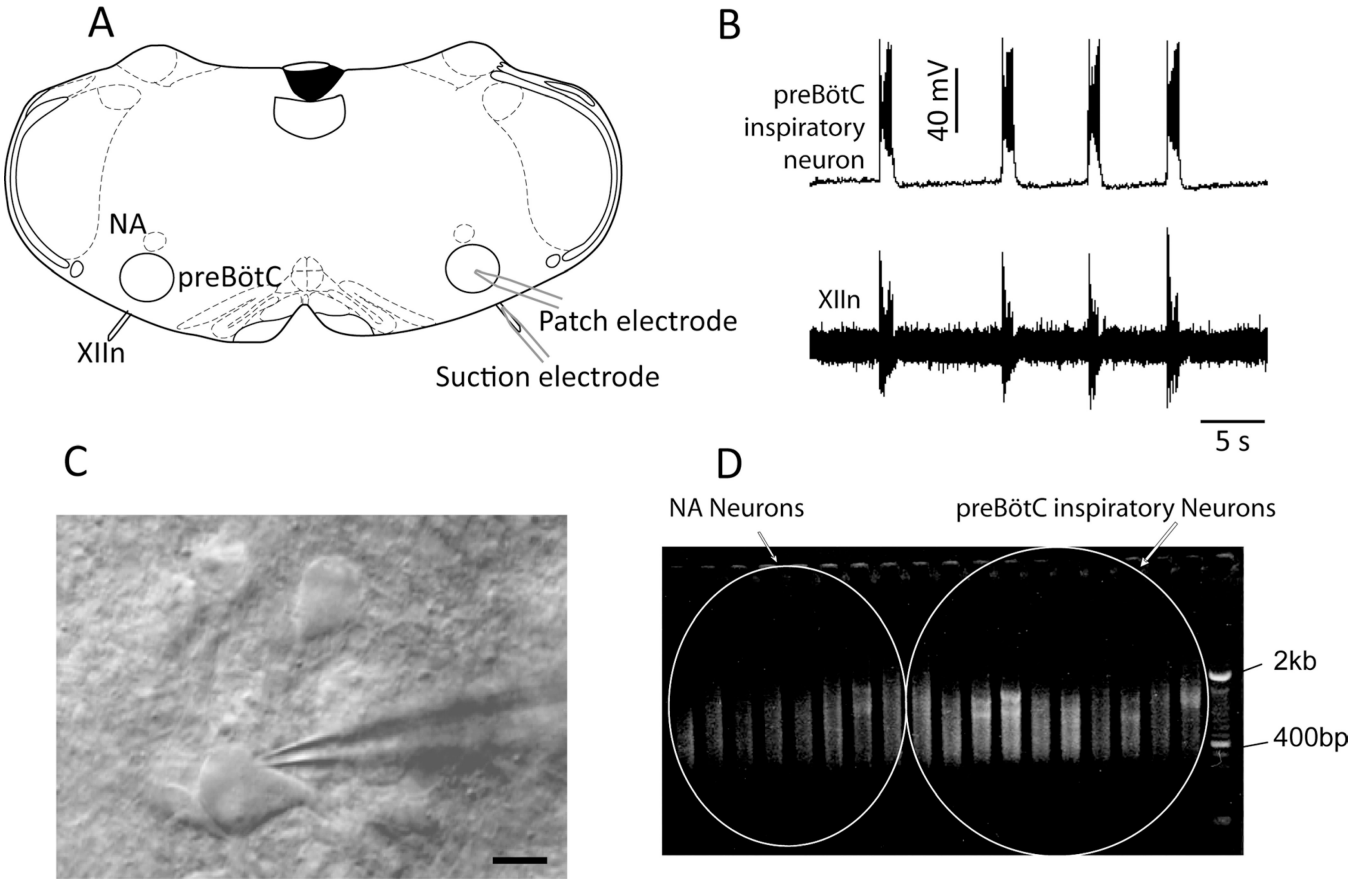

Figure 1.

RNA isolation and cDNA amplification from single inspiratory pre-BötC neurons. **A**: Outline of mouse medullary slice showing experimental setup. **B**: Typical inspiratory pre-BötC neuron identified by a burst of activity concurrent XII nerve output. **C**: Patch/ intracellular RNA aspirating electrode on inspiratory neuron viewed under infrared illumination. **D**: cDNA amplification from single neurons. Each lane represents cDNA enriched from a single pre-BötC inspiratory or NA neuron. NA, nucleus ambiguus; pre-BötC, pre-Bötzinger complex; XII, hypoglossal nucleus; XIIn, hypoglossal nerve. Scale bar = 10 μm.

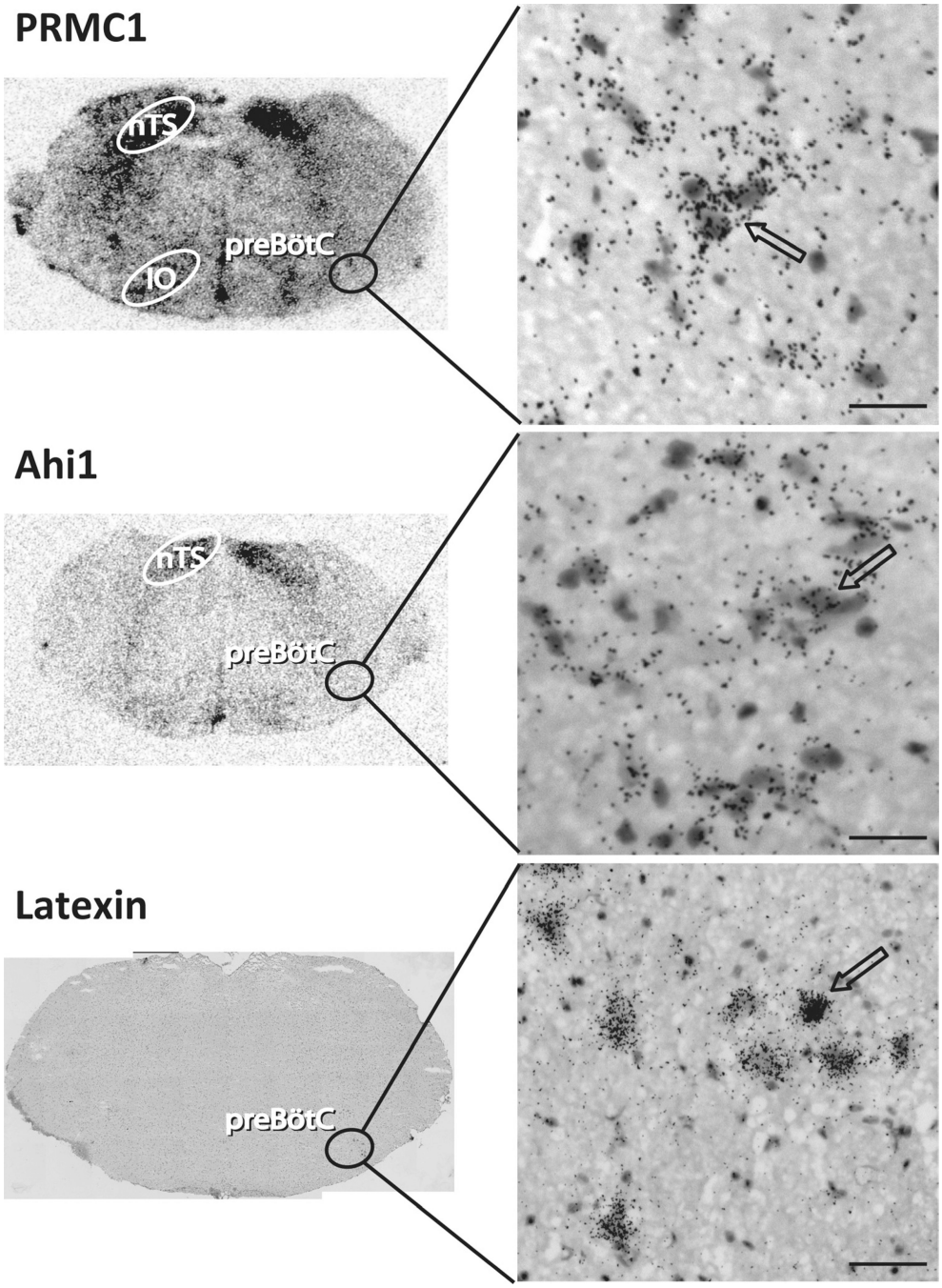

Figure 2.

Medullary expression pattern of *PRMC1*, *Ahi1*, and *Latexin* genes in pre-BötC using ^{35}S-radiolabeled RNA probes in brightfield photomicrographs. **Top**: PRMC1 is highly expressed in nucleus of the solitary tract (nTS), inferior olive (IO), and pre-BötC. **Middle**: Ahi1 is highly expressed in nTS and in pre-BötC. **Bottom**: Latexin is expressed in rostral pre-BötC and BötC (not shown). Counterstain: hemotoxylin- eosin. Left: Low-magnification of transverse medullary slice; right: high-magnification depicting pre-BötC. The arrows indicate labeled neurons. Scale bars = 30 μm.

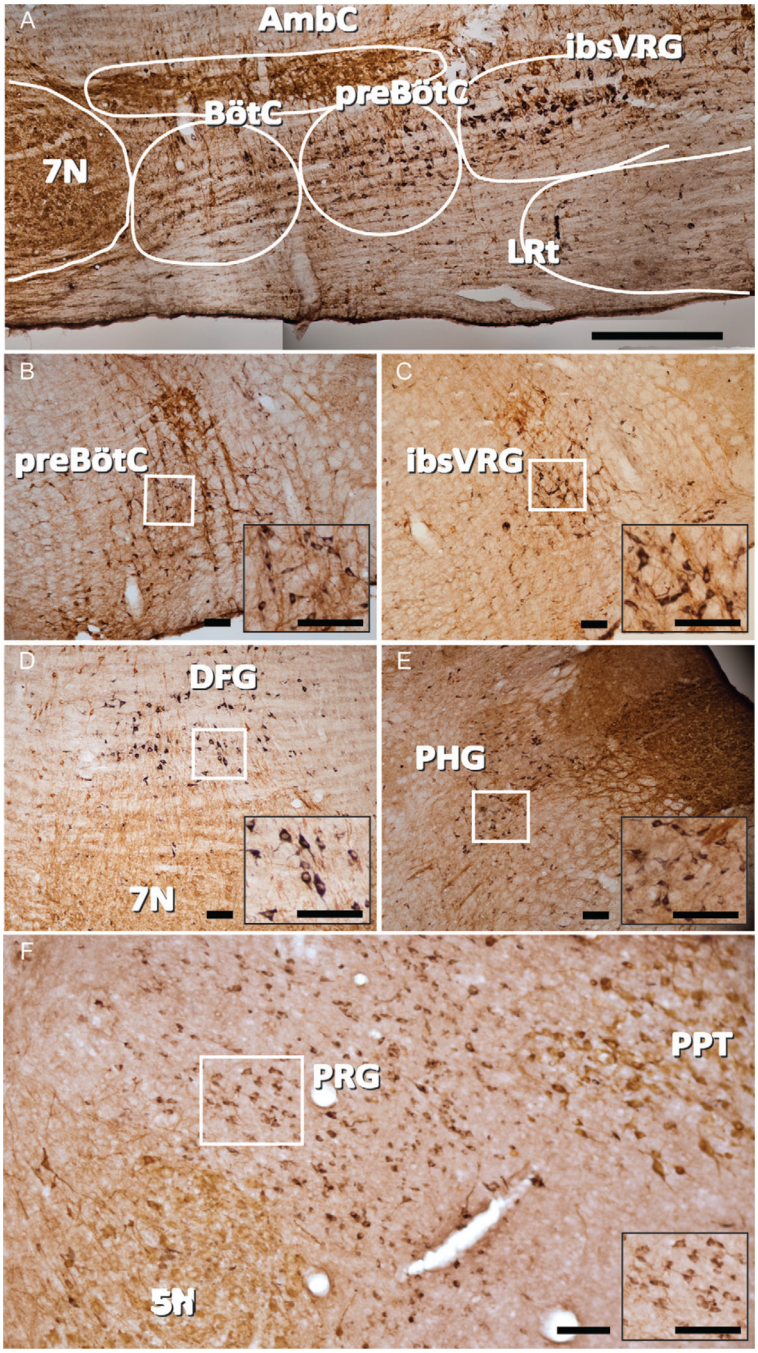

Figure 3.

Reelin expression in pre-BötC, ibsVRG, DFG, PHG, and PRG. **A**: Sagittal mosaic image of ventral respiratory column depicting reelin (black) and ChAT (brown) immunoreactivity. Double labeling with ChAT was used to reveal the motor neurons in the sections. **B**: Reelin neurons in pre-BötC in coronal section. **C**: Reelin neurons in ibsVRG in coronal section. **D**: Reelin neurons in PHG in coronal section. **E**: Sagittal view of the DFG. **F**: Sagittal view of the PRG depicting a band of reelin neurons between the trigeminal nucleus and the pedunculopontine tegmentum. **Insets** represent higher magnification of reelin-ir neurons from the boxed areas in each panel. BötC, Bötzinger complex; ibsVRG, inspiratory

bulbospinal ventral respiratory group; 5N, trigeminal nucleus; 7N, seventh nucleus; DFG, dorsal to facial nucleus group; PRG, pontine respiratory group; PHG, parahypoglossal group; PPT, pedunculopontine tegmentum. Scale bars = 500 μm in A; 100 μm in B–F. [Color figure can be viewed in the online issue, which is available at wileyonlinelibrary.com.]

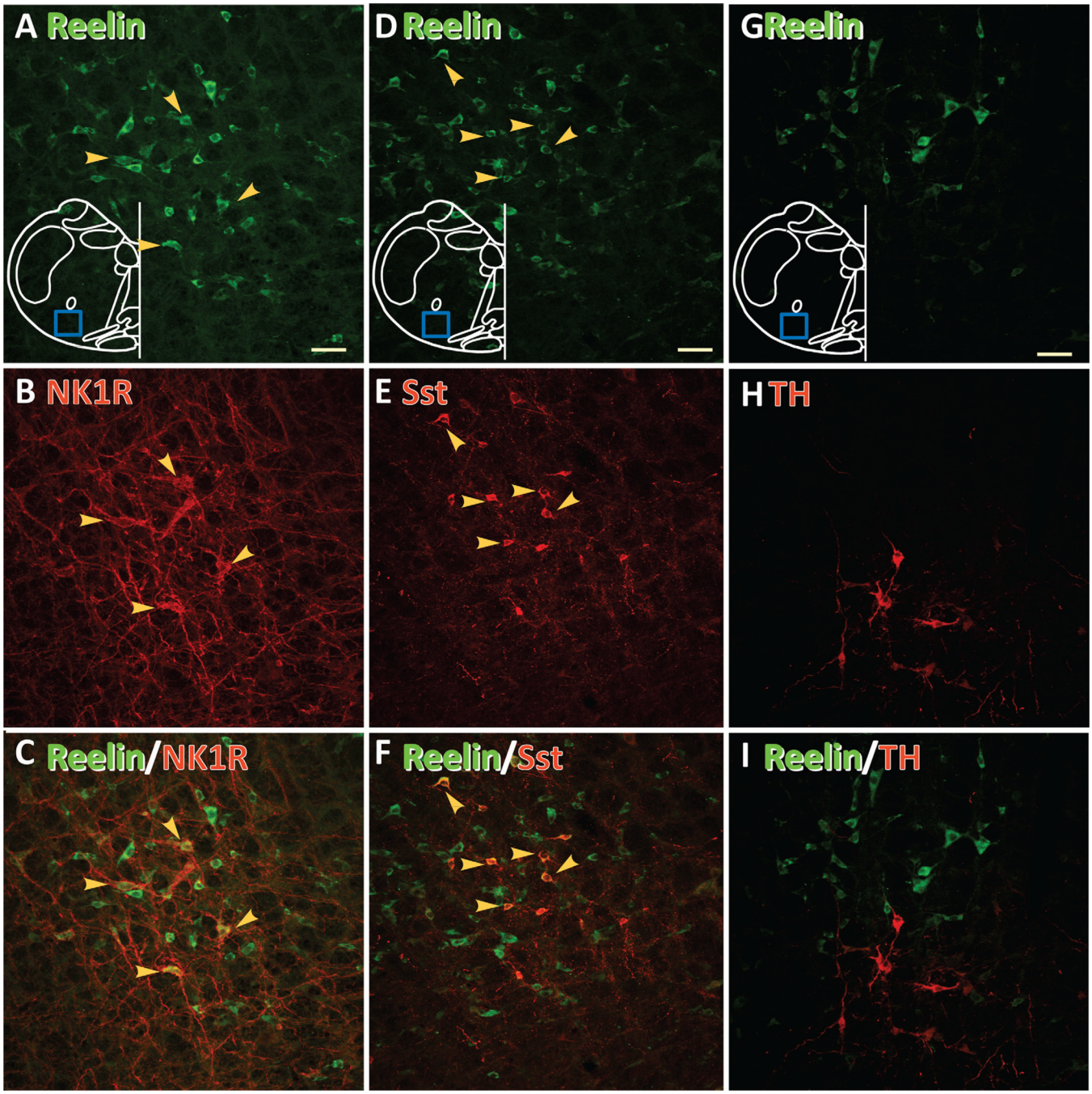

Figure 4.

Pre-BötC reelin neurons coexpress NK1R and Sst but not TH. **A,D,G**: Reelin neurons (green). The blue box represents the area including pre-BötC where image was acquired. **B**: NK1R neurons. **E**: Sst neurons. **H**: TH neurons. **C,F,I**: Superimpositions. Neurons colocalizating two markers indicated by yellow arrows. NK1R, neurokinin 1 receptor; Sst, somatostatin; TH, tyrosine hydroxylase. A magenta-green copy of this figure is available as Supporting Information Figure 1. Scale bars = 50 μm. [Color figure can be viewed in the online issue, which is available at wileyonlinelibrary.com.]

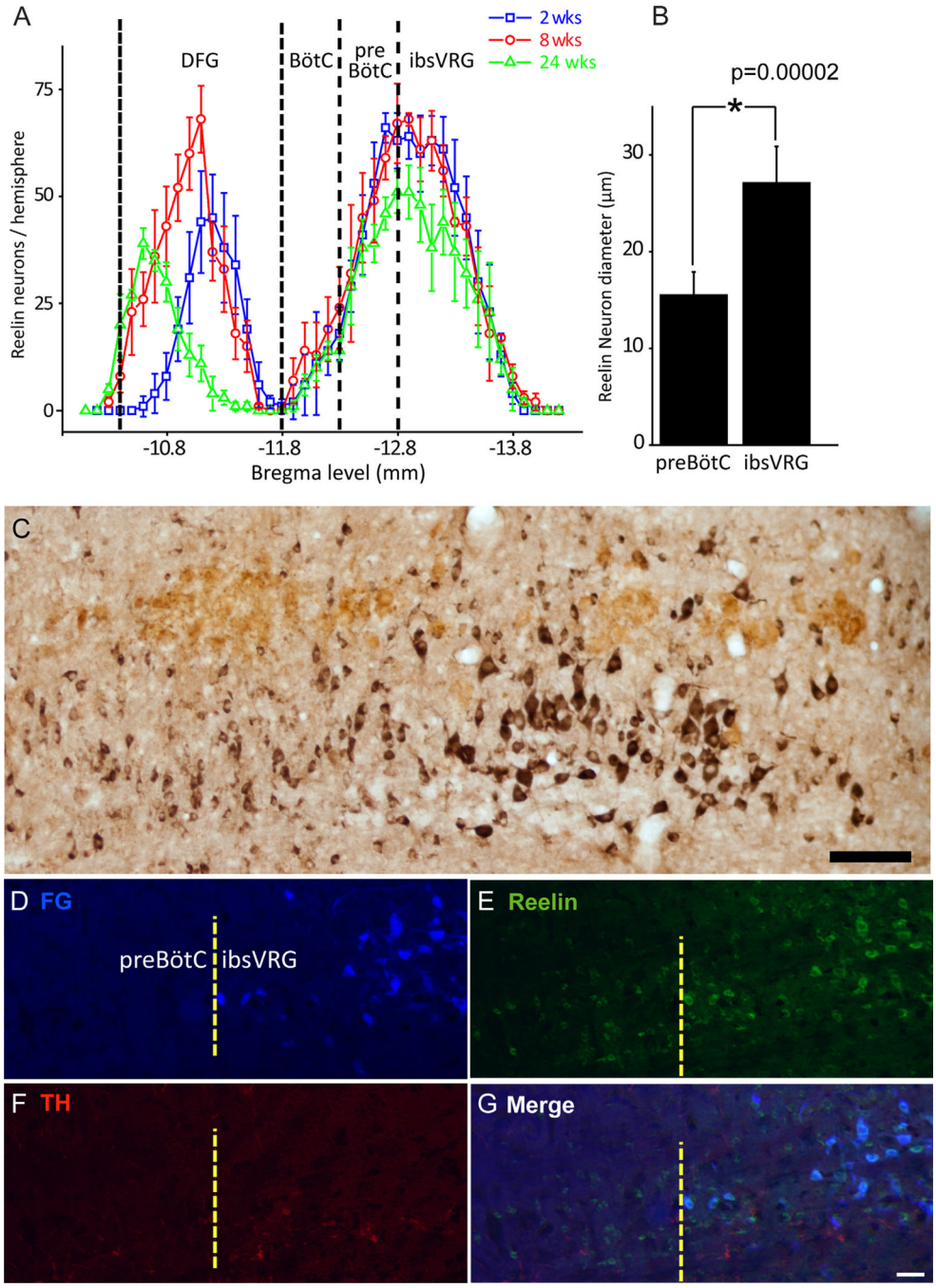

Figure 5.

Distinctive reelin populations set the anatomic boundary of pre-BötC and ibsVRG. **A**: Reelin neuron rostrocaudal distibution in ventrolateral medulla at three different ages. One reelin neuron group resides in the region from Bregma levels −10.4 to −11.7 mm in DFG; another reelin neuron group located in pre-BötC and ibsVRG with peak cell numbers from Bregma levels −12.7 to −12.9 mm. Caudal edge of the facial nucleus: Bregma −11.7 mm. **B**: Pre-BötC reelin neurons have significantly smaller soma diameter than those of ibsVRG (ANOVA, $P = 0.00002$). **C**: Sagittal view depicting pre-BötC and ibsVRG reelin populations, labeled for reelin (black) and ChAT (brown). Double label with ChAT was

used to reveal the motor neurons in the sections. **D–G**: ibsVRG neurons retrogradely labeled from the C2–C4 level of the spinal cord with FG (D) were stained for reelin (E) and TH (F). G: Merge. Note that FG-positive cells in ibsVRG are colocalized with reelin but do not express TH. ChAT, choline acetyltransferase; FG, Fluorogold; ibsVRG, inspiratory bulbospinal ventral respiratory group; TH, tyrosine hydroxylase. Scale bars = 100 μm in C; 50 μm in G (applies to D–G). [Color figure can be viewed in the online issue, which is available at wileyonlinelibrary.com.]

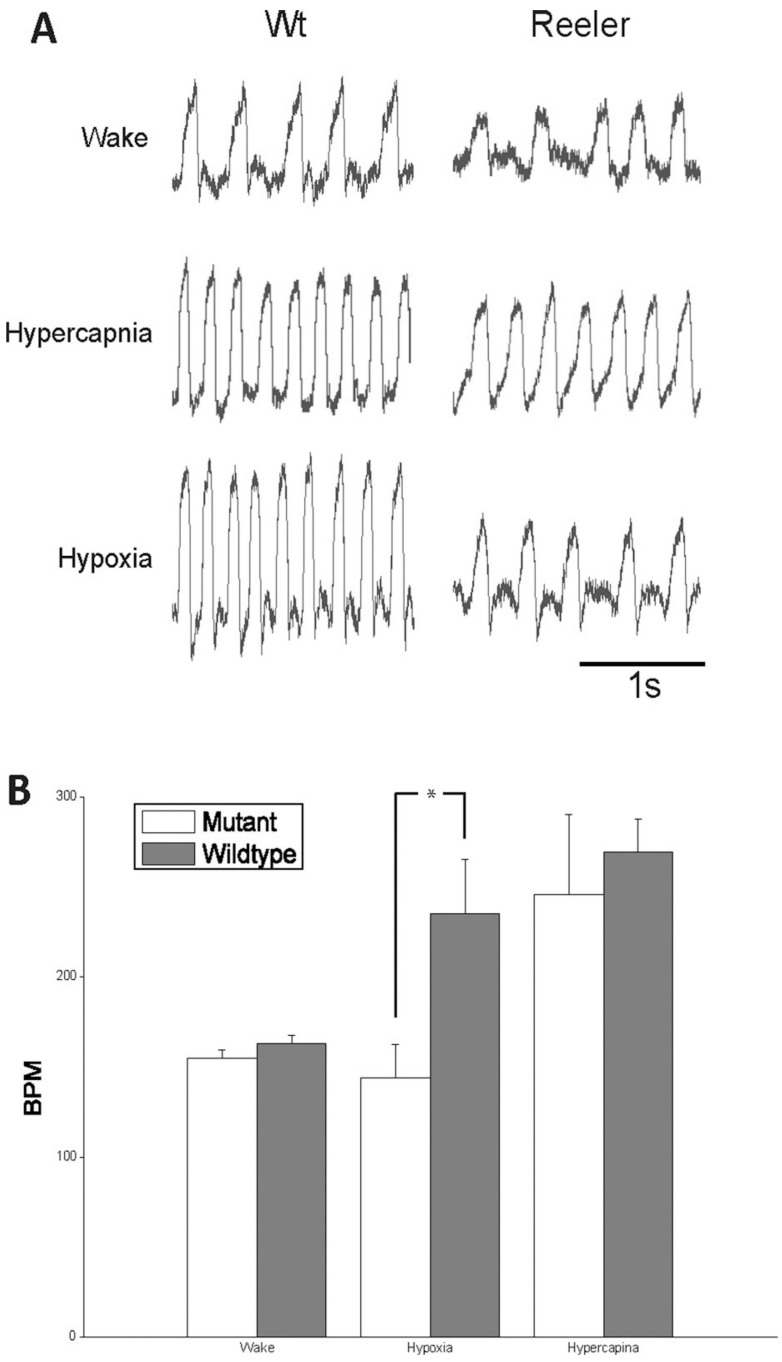

Figure 6.

Reeler mouse shows impaired response to hypoxia but not hypercapnia. **A**: Plethysmographic record of breathing patterns during wakefulness and hypoxic and hypercapnic challenges from Reeler and littermate control mice. Amplitudes are not normaliized. **B**: Quantitative analysis of breathing frequency from Reeler and littermate controls. Compared with littermates, Reeler mice had a significantly slower breathing frequency in response to hypoxia (ANOVA, $P = 0.0002$), which was not signficiantly different from baseline (ANOVA, $P = 0.501$). Values are mean ± SD (n = 5 for each group). BPM, breaths per minute.

TABLE 1

List of Partial Candidate Genes That Were Screened From a Subtractive cDNA Library of Single Inspiratory Pre-BötC Neurons

Gene name	Gene ID from Genbank
Abelson helper integration site (Ahi1) gene	gi|33392716|gb|BC055400.1|
Activin receptor A, type 1 (Acvr1)	gi|40254648|ref|NM_007394.2|
Agrin (Agrn)	gi|42490750|ref|NM_021604.2|
Armadillo repeat gene deleted in velo-cardiofacial syndrome (Arvcf)	gi|40254128|ref|NM_033474.2|
BM-009 homolog	gi|26344414|dbj|AK075613.1|
BM88, function unknown, or 1500001H12 gene	gi|31981113|ref|NM_021316.2|
BarH-like 1 (*Drosophila*) Barhl1	gi|255958264|ref|NM_019446.4|
Calcium modulating ligand (Caml)	gi|6671661|ref|NM_007596.1|
Corticotropin-releasing hormone (crh)	gi|45429989|ref|NM_205769.1|
Cyclin-dependent kinase4 (Cdk4)	gi|31560614|ref|NM_009870.2|
Estrogen-related receptor gamma (Esrrg)	gi|52345417|ref|NM_011935.2|
Exocyst complex component 7	gi|74150201|dbj|AK140450.1|
Glioma tumor suppressor candidate region gene 2	gi|74199027|dbj|AK151836.1|
Riken cDNA2900016C05 gene	gi|12850934|dbj|AK013532.1|,
G-protein-coupled receptor associated sorting protein1 (Gprasp1)	gi|53729356|ref|NM_026081.5|
G-protein-coupled receptor associated sorting protein 2 (Gprasp2), Predicted	gi|26081919|dbj|AK030638.1|
Hematopoietic signal peptide-containing membrane domain-containing 1	gi|54125558|gb|AY761098.1|
Hypothetical integrin A (or I) domain structure containing protein	gi|38174365|gb|BC061211.1|
Integral membrane protein 2B	gi|74207160|dbj|AK151889.1|
Kin of IRRE-like 3 (*Drosophila*), KIRRE, NEPH1	gi|38648724|gb|BC063072.1|
Latexin	gi|31980631|ref|NM_016753.2|
Membrane-associated ring finger (C3HC4) 4	gi|113865912|ref|NM_001045533.1|
Member T2 (Rhot2), Ras family	gi|34328359|ref|NM_145999.2|
Neuronal protein 3.1	gi|32451790|gb|BC054762.1|
Nulp1, bHLH family	gi|11036455|gb|U94988.1|MMU94988
PKI gamma	gi|20071652|gb|BC026550.1|
Progesterone receptor membrane component 1	gi|74198077|dbj|AK159599.1|
RAB4A, ras family	gi|74202132|dbj|AK136566.1|
Rho GDP dissociation inhibitor (GDI) alpha	gi|74217975|dbj|AK170718.1|
Reelin	gi|117320553|ref|NM_011261.2|
Riken cDNA 2900016C05 gene	gi|12850934|dbj|AK013532.1|
S100 calcium binding protein A10 (S100a10)	gi|113930762|dbj|NM_009112.2|
Solute carrier family 6 member 5 (Slc6a5)	gi|225579048|dbj|NM_001146013.1|
Tubulin tyrosine ligase-like family, member 6 (Ttll6)	gi|282847335|dbj|NM_172799.4|
Very KIND protein	gi|74181190|dbj|AK147335.1|
Visinin-like 1 (Vsnl1, NVL-1, NVP-1, HLP3)	gi|67514555|ref|NM_012038.3|
Zinc finger, DHHC domain containing 2 (Zdhhc2)	gi|31341589|ref|NM_178395.2|

TABLE 2

Antibodies Used in the Present Study

Antibody	Source	Immunogen	Dilution
Choline acetyltransferase (ChAT)	Chemicon, AB144 goat polyclonal	Human placental ChAT	1:500
Neurokinin 1 receptor (NK1R)	Advanced Targeting Systems, AB-N04, rabbit polyclonal	Synthetic peptide corresponding to 393–407 amino acid sequence of NK1R sequence at the C-terminus of dog NK-1 receptor	1:500
Reelin	Millipore, MAB5364, mouse monoclonal	Recombinant reelin amino acids 164–496	1:500
Somatostatin (Sst)	Peninsula Labs, T4103, rabbit polyclonal	H-Ala-Gly-Cys-Lys-Asn-Phe-Phe-Trp-Lys-Thr- Phe-Thr-Ser-Cys-OH	1:500
Tyrosine hydroxylase (TH)	Aves Labs, Inc., F1005, chicken polyclonal	Two peptides: RRQ SLI EDA RKE RE SDA KDK LR[N/S] YAS RIQ R	1:500